Emergent Scientist **9**, 1 (2025)

https://doi.org/10.1051/emsci/2024003

Emergent Scientist

Available online at:
https://emergent-scientist.edp-open.org

RESEARCH ARTICLE

OPEN ACCESS

# The value of hands-on experiments in an upper-division classical mechanics course

Steven W. Tarr[a], Joseph S. Brunner[a,b], Emily Alicea-Muñoz, and Daniel I. Goldman[*]

School of Physics, Georgia Institute of Technology, 837 State Street, Atlanta, GA 30332, USA

Received: 4 July 2024 / Accepted: 17 December 2024

**Abstract.** We share our experience incorporating open-ended experimentation into an upper-division classical mechanics course through project-based learning, including one student's investigation of a common textbook problem and its unexpected connections to astrophysics. By iterating a computational model and an experimental apparatus, the student participated in inquiry in a way that would not have been possible in a typical classical mechanics course. We advocate the adoption of similar hands-on approaches in the classroom to help upper-division students develop both an understanding of the value of experimentation and an appreciation of the diversity and subtlety of physical phenomena that can emerge in apparently simple systems.

**Keywords:** Project-based learning / classical mechanics / zoom-whirl orbit / experimental inquiry / simulation

## 1 Introduction

Many recent publications have focused on deviations between common exercises in the undergraduate mechanics classroom and corresponding experiments. These studies highlight how real-world physics regularly differs from the clean world of textbook problems across a variety of topics including uniform circular motion [1,2], rolling friction with and without slipping [3,4], and rotating reference frames [5,6]. Such studies also demonstrate the value and accessibility of simple tabletop experiments and simulations to an undergraduate mechanics audience. Providing students the opportunity to challenge their understanding by probing the limits of textbook mechanics principles may prove fruitful in further developing expert-like skills [7–11], beliefs [8,9], and self-confidence surrounding experimental physics [12–14].

We showcase an example of learning potential when instructors deliberately support student-led discovery in experimental physics outside the typical laboratory class setting. Through his work on a multiple-semester project derived from a standard upper-division classical mechanics problem, an undergraduate physics major discovered unexpected deviations from the typical classroom solution including the presence of zoom-whirl-like orbits and apsidal precession. Beyond deepening his appreciation for the diversity of phenomena that emerged from this seemingly simple system, the student learned design and fabrication methods for experiments and simulations, practiced oral and written science communication skills, and studied mathematical analysis techniques ahead of his academic degree schedule. We describe the iterative procedure followed to build, analyze, and understand the system, and advocate this process as a means of cultivating and empowering young experimental physicists in upper-division courses.

## 2 Method

### 2.1 Initial experiment

We adapted Example 2.9 in *An Introduction to Mechanics*, 2nd edn. by Kleppner and Kolenkow, which uses a mass-string system to teach students about rotational motion, translational motion, and constraints [15]. The system consists of a frictionless horizontal table with a hole through its center (Fig. 1a). Mass A ($M_A$) sits atop the table and is attached to a hanging Mass B ($M_B$) by an inextensible string of length $\ell$ running through the central hole. While $M_A$ rotates at a fixed radius $r$, $M_B$ is held at a fixed height $z$. At a later time, $M_B$ is released, and the

[*] e-mail: daniel.goldman@physics.gatech.edu
[a] These authors contributed equally to this work.
[b] Currently at Department of Radiation Medicine, University of Kentucky – 800 Rose Street, Lexington, KY 40536, USA.

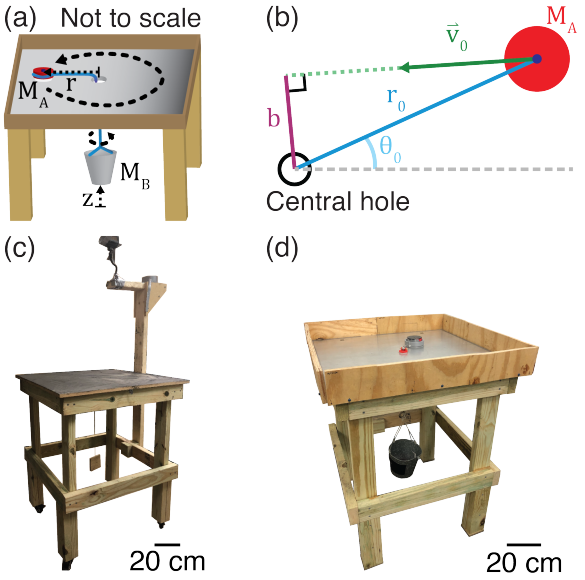


**Fig. 1.** Textbook mass-string system. (a) Diagram of physicalized mass-string system inspired by Example 2.9 in reference [15]. (b) Example initial conditions for $M_A$. (c) Original and (d) final experimental apparatuses. Curtains are removed from (d) for increased visibility of $M_B$.

system evolves. Readers are asked to find the instantaneous acceleration of $M_B$.

The initial experimental apparatus consisted of a $76 \times 76 \times 86$ cm$^3$ wooden table (Fig. 1c). We sanded the tabletop to decrease friction and drilled a central hole through which we ran a 5.4-kg-capacity monofilament fishing line. The line had length $\ell = 48$ cm such that it remained permanently taut and $M_B$ could only collide with the ground when $r = 0$. We spread powdered graphite on the tabletop to decrease the coefficient of kinetic friction to a measured value of $\mu = 0.22$. An $M_A = 321$ g metal shuffleboard puck and a pail filled with blocks of varying masses functioned as $M_A$ and $M_B$ respectively.

After placing the puck in its initial position, a spring-loaded trigger underneath the table locked the fishing line, preventing the system from evolving. A weighted pendulum attached to the table hit the puck, with the initial pendulum angle determining the puck's initial speed. Mimicking the textbook problem, we restricted the initial conditions to a strictly angular velocity. The trigger released at the moment the pendulum hit the puck, allowing the system to evolve. A 250-fps smartphone camera recorded a top-down view of the puck trajectories for tracking and analysis in Matlab.

## 2.2 Simulation

To better mimic the physical apparatus, we modified the equations of motion in the textbook, incorporating both sliding friction and the constraint equation $z = r$:

$$\ddot{r} = \frac{M_A r\dot{\theta}^2 - M_B g}{M_A + M_B} - \frac{M_A}{M_A + M_B}\frac{\mu g \dot{r}}{\sqrt{\dot{r}^2 + r^2\dot{\theta}^2}} \quad (1)$$

$$\ddot{\theta} = -\frac{2\dot{r}\dot{\theta}}{r} - \frac{\mu g \dot{\theta}}{\sqrt{\dot{r}^2 + r^2\dot{\theta}^2}}, \quad (2)$$

where $\theta$ is the azimuthal angle of $M_A$ from its initial position and $g$ is the gravitational acceleration. We also recast $M_A$'s initial velocity $\vec{v}_0 = \left\langle \dot{r}_0, r_0\dot{\theta}_0 \right\rangle$ in terms of the impact parameter $b$ and initial speed $v_0 \equiv |\vec{v}_0|$. Here, $b$ describes the perpendicular distance from the center of the table to the line tangent to $\vec{v}_0$ (Fig. 1b):

$$v_0^2 = \dot{r}_0^2 + r_0^2\dot{\theta}_0^2 \quad (3)$$

$$b = r_0 \sin\left[\arctan\left(\frac{r_0\dot{\theta}_0}{\dot{r}_0}\right)\right] \quad (4)$$

$$\Rightarrow \vec{v}_0 = \left\langle \pm\frac{v_0}{r_0}\sqrt{r_0^2 - b^2}, \pm\frac{v_0 b}{r_0} \right\rangle. \quad (5)$$

We created a numerical simulation of equations (1) and (2) in Matlab that plots puck trajectories using inputs for parameters $b$, $r_0$, $v_0$, $M_A$, $M_B$, and $\mu$. Simulations terminated when $M_A$ contacted a boundary or after a fixed iteration period, whichever came first. The simulation permitted the study of trajectories with arbitrary $\vec{v}_0$, allowing us to expand upon the exclusively tangential $\vec{v}_0$ described by the textbook. Additionally, the simulation enabled a more efficient parameter sweep and removed the physical restrictions on parameter choices such as heavy masses, high initial speeds, and varied coefficients of friction. By matching initial conditions between experiment and simulation, we observed qualitatively consistent trajectories often characterized by low-eccentricity, decaying, elliptical spirals (Fig. 3).

Having established an approximate agreement between experiment and simulation, we fixed $\mu = 0.22$ per prior measurement and probed a variety of parameter choices in simulation. Most initial conditions yielded either decaying spiral orbits or trajectories terminating at a table boundary without completing a single revolution. Rarely, parameter choices resulted in a radial plunge. Having observed qualitative similarity between trajectories with highly varied initial conditions, we suspected that friction dominated the puck dynamics and elected to probe a reduced-friction simulation.

Simulations of frictionless ($\mu = 0$) and near-frictionless ($0 < \mu \leq 0.06$) puck-table interactions demonstrated rich dynamics with precessing orbits and deflections greater than 360° akin to those found in general relativity (GR). In the spirit of analogy, we borrow established terminology from astrophysics and GR when describing our system's dynamics [16]. In this new regime, puck trajectories often appeared as a finite number of "leaves" circulating about the center hole (Fig. 2). Consecutive leaves were typically separated by one or more higher-velocity, low-radius revolutions and sometimes demonstrated apsidal precession depending on initial conditions. We note the similarity between our observed orbits and the well-known "zoom-whirl" orbits around rotating black holes, albeit with far fewer whirls than established astrophysical results [16,17].

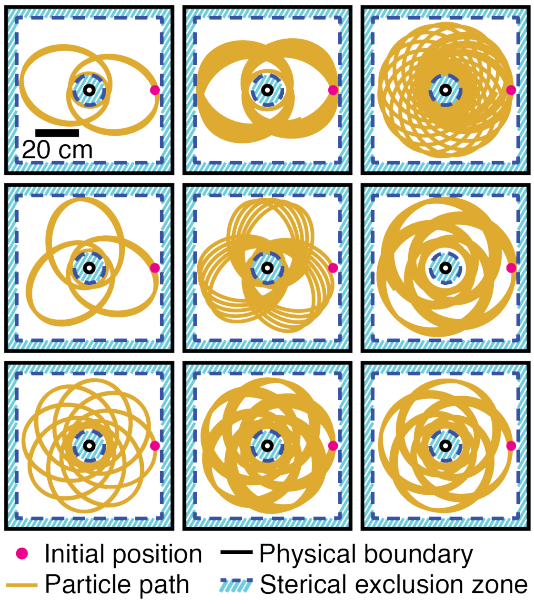


**Fig. 2. Simulated frictionless trajectories**. A variety of trajectories simulated from equations (1) and (2) for parameter choices $\mu = 0$, $r_0 = 30$ cm, $M_A = 0.32$ kg, and simulation time $t = 9$ s. Despite the classical nature of the mass-string problem, simulated trajectories resemble astrophysical orbits with small-orbital-radius revolutions separating apoapsides, $n$-fold symmetries, and apsidal precession.

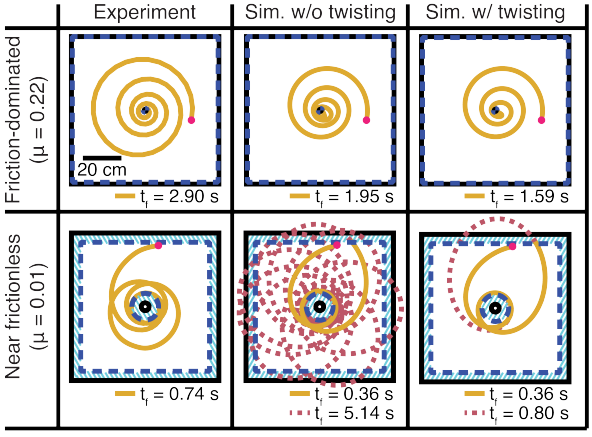


**Fig. 3.** Evolution of experiment-simulation comparison. Trajectories and completion times $t_f$ for initial and final apparatuses with corresponding simulations without and with line-twisting behavior. Dotted red lines show simulation results without the outer boundary. Unbounded simulations with twisting come closest to experiments. Friction-dominated trial parameters: $M_A = 0.32$ kg, $M_B = 0.51$ kg, $r_0 = 24$ cm, $b/r_0 = 1.00$, $v_0 = 1.9$ m/s. Near-frictionless trial parameters: $M_A = 0.36$ kg, $M_B = 5.3$ kg, $r_0 = 31$ cm, $b/r_0 = 0.89$, $v_0 = 2.8$ m/s. Experiments shown in Movie S1.

Zoom-whirl orbits occur when $q \equiv T_r/T_\phi > 1$, where $T_r$ is the time between successive apoapsides (i.e., farthest points from central body per revolution) and $T_\phi$ is the time to complete a single revolution averaged over the path between successive apoapsides [16,17]. In our simulation, we found $q$ decreased below one and eventually became undefined with increasing $\mu$ and decreasing $M_B$ regardless of other parameter choices. These low-friction and high-central-potential requirements for zoom-whirl behavior are suggestive of astrophysical regimes. With the emergence of zoom-whirl-like behaviors in our classical system, we chose to attempt to reproduce in the experiment elements resembling hallmarks of GR (e.g., central force, apsidal precession, zoom and whirl behaviors) in pursuit of a possible analogy. As these desired elements vanished in simulations of the frictional regime, we iterated our apparatus (Fig. 1d) to minimize friction ($\mu = 0.01$) and expand its capabilities to match the parameter sweep performed in simulation (see Section 5).

### 2.3 A twist on textbook mechanics

Following some trials in experiment that terminated with $M_A$ colliding with the center hole, we observed $M_B$ spinning rapidly, often leading to $M_A$ spontaneously accelerating and circling the center hole. Unexpectedly, the puck's initial angular motion torqued the fishing line, causing it to twist under the table. As the line twisted, it stored kinetic energy; once the system reached zero angular momentum (usually by colliding with the center hole), the line untwisted and reintroduced the stored energy, leading to the rapid acceleration of both masses.

To account for this behavior, we modified our simulation by modeling the twist as a mid-trial shortening of the line with a corresponding increase in the system's potential energy $U$ like that of a torsional spring [18]:

$$\ell'^2 = \ell^2 - R_\ell^2 \phi^2 \tag{6}$$

$$z = r + \ell - \ell' \tag{7}$$

$$U = M_B g z + \frac{1}{2}\kappa\phi^2. \tag{8}$$

Here, $\ell'$, $\ell$, $R_\ell$, $\phi$, and $\kappa$ are the line's contracted length, rest length, radius, twist angle, and coefficient of torsion (measured to be $\kappa = 0.0015 \pm 0.0001$ N·m·rad$^{-1}$) respectively. We coupled the twist to both masses' positions by introducing the following constraints:

$$\phi \equiv \theta - \Theta \tag{9}$$

$$\Theta_0 = \theta_0, \tag{10}$$

where $\Theta$ is the azimuthal rotation angle of $M_B$. In turn, we updated the system's kinetic energy $K$ to account for the spinning $M_B$:

$$K = \frac{1}{2}M_A\left(\dot{r}^2 + r^2\dot{\theta}^2\right) + \frac{1}{2}M_B\dot{z}^2 + \frac{1}{2}I_B\dot{\Theta}^2, \tag{11}$$

where $I_B = \frac{1}{2}M_B R_B^2$ is the moment of inertia of the approximately cylindrical $M_B$ with radius $R_B$. Finally, we accounted for typical sliding friction with the following dissipation function:

$$D = \mu M_A g\sqrt{\dot{r}^2 + r^2\dot{\theta}^2}. \tag{12}$$

Given equations (6)–(12), the solutions to the Euler-Lagrange equations yield the revised equations of motion.

$$\ddot{r} = \frac{1}{M_A v_A \ell' \gamma}\Big(M_A M_B \ell' R_\ell^2 r^2 \phi^2\Big(v_A \ell' \kappa - M_A \beta R_\ell^2\Big) - I_B M_A \ell'\Big(M_A \beta \ell'^2 r^2 + \mu M_B g R_\ell^2 \phi\big(R_\ell^2 \dot{r}\phi - \ell' r^2 \dot{\theta}\big)\Big) + I_B M_B v_A \ell' R_\ell^2 \phi\Big(\ell' \kappa \phi + M_A r\big(2\ell' \dot{r}\dot{\theta}^2 + g r \phi + R_\ell^2 \dot{\theta}^3 \phi\big)\Big) - I_B M_A M_B v_A \ell^2 r^2\Big(g\ell' + R_\ell^2 \dot{\phi}^2\Big)\Big) \tag{13}$$

$$\ddot{\theta} = \frac{1}{M_A v_A \ell'^2 \gamma}\Big(I_B \phi\Big(\beta \ell'^3 + g v_A \ell' \ell^2 - M_T v_A \ell'^4 \kappa - M_A M_B R_\ell^2\Big(v_A R_\ell^2\big(g\ell'\phi^2 + \ell^2 \dot{\phi}^2\big)\Big)\Big) - I_B M_A M_T \alpha \ell'^4 r \dot{\theta} - M_A^2 M_B \alpha \ell' R_\ell^4 r \dot{\theta} \phi^2\Big) \tag{14}$$

$$\ddot{\Theta} = \frac{1}{v_A \ell'^2 \gamma}\Big(M_T v_A \ell'^2 \kappa r^2 \phi - M_A M_B R_\ell^2 r \phi\Big(\alpha \ell'^2 \dot{\theta}\phi + \ell' r\big(\beta \ell'^2 - g v_A \ell^2\big) + v_A R_\ell^2 r\big(g\ell'\phi^2 - \ell^2 \dot{\phi}^2\big)\Big)\Big) \tag{15}$$

We simplify these complex equations by making physically motivated definitions for both $M_A$'s instantaneous velocity $v_A \equiv \sqrt{\dot{r}^2 + r^2\dot{\theta}^2}$ and the total mass $M_T \equiv M_A + M_B$. We also define the following for ease of reading: $\alpha \equiv \mu g r + 2 v_A \dot{r}$, $\beta \equiv \mu g \dot{r} - v_A r \dot{\theta}^2$, and $\gamma \equiv M_B R_\ell^4 \phi^2 \left(I_B - M_A r^2\right) - I_B M_T \ell'^2 r^2$. The simplified equations of motion are shown in equations (13)–(15).

With the addition of twisting, simulated trajectories shortened significantly and showed improved qualitative resemblance to experimental results. Orbits that once demonstrated long-lived apsidal precession instead terminated rapidly at the central hole (Fig. 3). We liken the effect of twisting to that of a capacitor in a circuit where $\kappa$ fills the role of inverse capacitance. As the puck revolves around the central hole, its kinetic energy is stored as potential energy in the twisted line. When the system's inertia can no longer overcome the torsional restoring force, the line untwists and reintroduces the energy as a rapid acceleration of both masses. Since our line has small $\kappa$ and trajectories were short-lived, we always observed untwisting to occur after the termination of an orbit at a boundary. As a result, the twisting behavior functionally acts as a form of dissipation where dissipated energy is only reintroduced after the completion of a trial.

## 3 Results

### 3.1 Experimental results

With the inclusion of line-twisting, we swept three parameters $M_B$, $v_0$, and $b/r_0$ in Matlab for typical values of $\mu$, $M_A$, and $r_0$ (0.01, 0.35 kg, and 0.28 m respectively) such that we might narrow our experimental search for zoom-whirl behavior. For parameter combinations that produced long-lived trajectories, an increase in $M_B$ yielded a proportionate increase in $q$ (Fig. 4). Having observed a similar trend in experiment, we consequently fixed $M_B = 5.3$ kg at the maximum safe value for our apparatus. Varying the remaining parameters in simulation, we observed two further conditions requisite for $q$ to be defined: (1) $b/r_0 \geq 0.98$, and (2) $v_0 \in [2.5, 6]$ m/s (Fig. 5a). When both inequalities are satisfied alongside the maximal $M_B$, the resultant trajectories always qualify as zoom-whirl (i.e., $q > 1$). Should either condition fail to be met, $M_A$'s trajectory swiftly terminates at a boundary.

Guided by the slice of parameter space in Figure 5a, we targeted similar values of $v_0$ and $b/r_0$ in experiment (Fig. 5b). Experimental trajectories exhibited larger dissipation than those in simulation with identical parameters, causing more rapid termination at the central hole. Orbits often possessed a single apoapsis, resulting in an undefined $q$. Without $q$ to guide our understanding in experiment, we turned to the winding angle $\theta_w$ (i.e., angular displacement of $M_A$) as an alternative representation of trajectory shape. By separately varying $v_0$ and $b/r_0$, we performed a sensitivity analysis of $\theta_w$ (Figs. 5c, 5d). In both experiment and simulation, we observed intermediate $v_0$ and high $b/r_0$ to be most successful at creating long-lived, zoom-whirl-like orbits.

Often, $\theta_w$ was larger in experiment than in simulation. We attribute this result to the interplay between our choice of $r_0$ and boundary conditions. Though trials with larger $r_0$ typically led to longer trajectories in our apparatus, the apparent reduction of dissipation in simulation resulted in trajectories with matching $r_0$ that regularly terminated at the outer boundary. By removing the outer boundary in simulation, conditions that already generated large $\theta_w$ saw a further increase and often compared favorably with experimental results. (Figs. 5c, 5d). We speculate that further investigation into modeling unaccounted sources of dissipation would collapse the curves from both simulations and create a more favorable comparison to experiment.

## 4 Discussion

### 4.1 Experimental takeaways and professional development

In performing a hands-on investigation, the undergraduate student directly observed the behavior of a system previously confined to a textbook example. The construction of the apparatus highlighted the non-physical components of the text and how the dynamics change upon physicalizing the system. For example, the line twisted as the puck orbited, storing energy and greatly

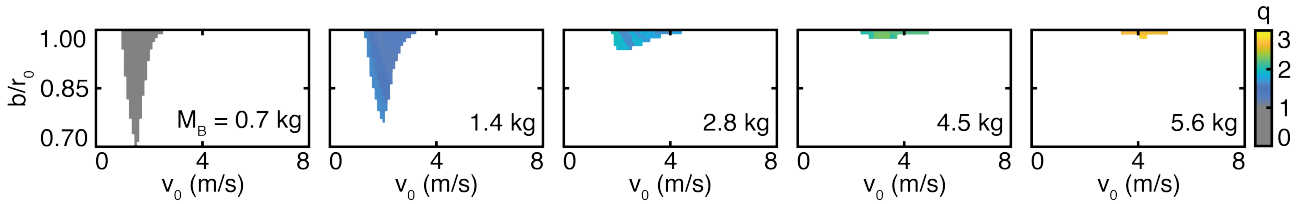


**Fig. 4.** Simulated parameter space. Parameter-space heatmaps of $q$ (i.e., the ratio of the time between successive apoapsides to the average time to complete a revolution [16,17]) from simulation for typical values $\mu = 0.01$, $M_A = 0.35$ kg, and $r_0 = 0.28$ m. White space corresponds to short trajectories with undefined $q$. Simulated orbits become more zoom-whirl-like as the central force increases. However, a larger $M_B$ also results in more frequent crashes with boundaries, leading to a significant size reduction of parameter space with defined $q$.

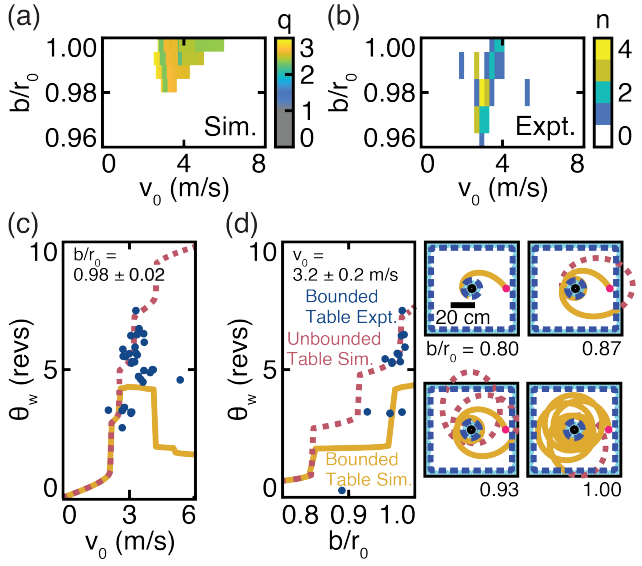


**Fig. 5.** Zoom-whirl sensitivity. (a) Parameter-space heatmap of $q$ from simulation for chosen experimental values $\mu = 0.01$, $M_A = 0.35$ kg, $r_0 = 0.28$ m, and $M_B = 5.3$ kg. For these parameter choices, all long-lived trajectories qualify as zoom-whirl orbits. (b) Parameter-space histogram of experimental trials with target combinations informed by (a); $n$ describes the number of trials per combination. (c, d) Sensitivity analysis of $\theta_w$. Simulated trajectories on a finite table often terminate at the outer boundary; those on an infinite table must terminate at the central boundary. Larger dissipative effects observed in experiment quickly draw $M_A$ away from the outer boundary, creating orbits that exclusively terminate at the central boundary. (*Outset*) Archetypal simulated trajectories demonstrate the discontinuous nature of the sensitivity plots with qualitatively distinct orbits.

altering trajectories. Additionally, tabletop friction was significant in characterizing trajectories; its minimization even led to imitation zoom-whirl orbits (Fig. 3) similar to those in reference [17]. A student reading the textbook or working the problem on paper is unlikely to anticipate these complex behaviors stemming from simple but subtle origins.

Despite the substantial evolution of both the apparatus and model toward compatibility, there were still notable deviations between experimental and simulated trajectories. Orbits in the experiment rarely persisted for more than one second and never exhibited more than one apoapsis, standing in sharp contrast to the simulated parameter space with multiple apoapsides (Fig. 5a). These discrepancies suggest there may be additional forms of dissipation in the physical experiment that have not been considered. For example, as the student examined greater $v_0$ and $M_B$, the apparatus began shaking in response to the system's large internal forces. We postulate that modifying the simulation to account for the inertial forces and energy dissipation incurred by this shaking would reduce the differences between experiment and simulation.

Beyond piloting the research and resultant discoveries described above, the student also engaged in significant professional development outside the scope of the traditional undergraduate physics curriculum. In the process of physicalizing a textbook problem, the student developed an experiential understanding of the realities of complex dynamical systems; their design, fabrication, and iteration processes; and how they are studied in experimental research labs. The student increased his mathematical abilities by learning and applying the Lagrangian formulation of classical mechanics a semester ahead of the degree schedule, and he improved his computational skills by simulating the system in Matlab. Finally, the student improved his oral and written communication skills by presenting his results at a conference [19] and participating in the writing of this paper.

### 4.2 Broader pedagogical significance

It is often necessary to make simplifying assumptions when teaching undergraduate classical mechanics. For example, in Kleppner and Kolenkow's version of the system, friction is deemed negligible, the connecting line is nonphysical (i.e., massless, one-dimensional, inextensible), and the platform upon which $M_A$ rests is an infinite plane with no physical presence aside from a normal force to constrain $M_A$'s $z$-coordinate [15]. Within this context, we frequently present "simple" mechanical systems as "solved" so that students can develop an intuition for how dynamical systems should behave. And although this is undoubtedly a necessary tool for guiding learners toward foundational understanding, the simplifying assumptions required for a textbook solution can hide interesting phenomena that go against expectations, giving students the impression that classical mechanics is "dull." Much like other recent publications [1–6], our research points in

the opposite direction: open-ended tabletop experiments and simulations may provide students with a glimpse at the diversity of phenomena that can emerge in "simple" nonlinear systems.

When adapting textbook problems for classroom experiments, students and instructors often must grapple with long-instilled simplifying assumptions. For example, when friction is incorporated into a formerly frictionless problem, the most common preconception is that there will be energy dissipation that hinders any existing motion [20]. Likewise, in constructing a physical version of Kleppner and Kolenkow's frictionless system, we expected the textbook problem's perfectly circular orbits would dampen into decaying spiral trajectories terminating at the tabletop's central hole. Though we indeed observed decaying spirals in our original, highly frictional apparatus, iterating the system to be near-frictionless revealed unexpected dynamics. In both simulation and experiment, the purely classical mass-string system demonstrated tangible astrophysical connections in apsidal precession and zoom-whirl behavior when approaching the frictionless regime. In adopting the commonplace assumptions on how dissipation affects a dynamical system, we failed to consider the possibility that such dynamically rich phenomena could emerge in what we believed to be a simple system. Similarly, students who lack experience in open-ended inquiry may miss the insight that comes from taming messy results through iteration. When leading students through activities involving simplifications, we must tread carefully and be explicit about the limitations of the approach so students assume neither that all dynamical systems can be easily solved nor that the initial chaos of an experiment is forever inscrutable.

## 5 Dead end

The most significant dead ends we encountered involved the initial experimental apparatus. The zoom-whirl orbits produced in simulation required faster $v_0$, heavier $M_B$, non-tangential $\vec{v}_0$, and a near-frictionless tabletop. Without the following modifications, our apparatus exclusively produced decaying spiral and radial plunge trajectories.

The original fishing line regularly broke under increased tension from larger $v_0$ and $M_B$; a replacement line with 136-kg capacity was sufficient for subsequent experiments. Since the $M_A$-launching pendulum confined experiments to a strictly tangential $\vec{v}_0$, we instead launched $M_A$ by hand and determined initial conditions in post using Matlab (Fig. 5b). The thin, tabletop layer of graphite powder reduced friction insufficiently for zoom-whirl orbits. Inspired by a classroom video wherein a flea pulls one million times its body mass in near-frictionless weights [21], we replaced the shuffleboard puck with a 6-cm-tall, 6.4-cm-diameter dry ice puck. A 3D-printed helmet lined with foam and lead insulated the puck and kept it from toppling during experiments. Further, we replaced the graphite with a galvanized aluminum sheet to increase the dry ice's sublimation rate and consequently decrease the effective coefficient of friction. Taken altogether, these adjustments to the apparatus yielded a new $\mu = 0.01$, a 95% decrease from the original apparatus.

Despite obtaining a near-frictionless interaction between the dry ice puck and the table, we observed experimental trajectories terminate at a boundary in less time than simulated trajectories with matching initial conditions. During preliminary experiments, we observed the monofilament line scrape the edge of the center hole. To address this additional source of friction, we affixed a plastic ball bearing (McMaster part 6455K37) in the center hole and mounted a pulley bearing (McMaster part 3434T21) on a 3D-printed swivel, each with an estimated $\mu$ between 0.0010 and 0.0015 [22]. As the puck moved, the line spun over the pulley and the swivel rotated inside the ball bearing, minimizing friction in $\hat{r}$ and $\hat{\theta}$ respectively. Experimental trajectories persisted longer as a result, suggesting less energy was dissipated by friction against the line.

## 6 Conclusion

In the classroom, the "thought experiment" is a powerful tool for strengthening one's understanding of physics principles. An instructor may present their students with the concept of the mass-string system and ask probing questions about constraint equations, Newton's Laws, and rotational motion, allowing students the opportunity to exercise their mental muscles on each of these topics. And yet, when we mentally play with a thought experiment, we can only tinker with what we already know to be factors of the system dynamics. We play in a wholly nonphysical way, and so we limit ourselves by our creativity. If the problems we teach were truly simple and thoroughly understood, then there would be no issue with limiting ourselves to learning mechanics through thought alone.

In our study, we directly confronted the limitations of this approach. In building the mass-string system, we observed unexpected behaviors in line-twisting and table-shaking, both of which were dynamically significant and led to dramatic deviations between the simulated equations of motion and experiment. Although these behaviors may seem obvious in hindsight, it is unlikely that students would account for all important sources of deviation between the physical system and the problem by simply reading the text. Thought experiments are tremendously valuable, but they do not provide a comprehensive approach to learning physics. Hands-on experimentation can help, but few courses offer learning through physical experiments and even fewer boast open-ended inquiry [23]. As a result, students often miss crucial opportunities to develop expert-like experimentation skills, agency, and physics intuition. By allowing students to engage in tactile learning via tabletop science projects in research-lab-style settings, we give students the opportunity to identify gaps in their knowledge and gain significant physics insight.

### Acknowledgments

We thank Daniel Soto and Andras Karsai for help updating the apparatus and data pipeline. We thank Shengkai Li for

helpful discussions on GR. We thank Prof. Michael Schatz and Dr. Edwin Greco for helpful discussions on pedagogy. We thank Prof. Brian Hammer for supplying proper storage for dry ice pucks. This work was funded by a Dunn Family Professorship (author DIG) and the Georgia Institute of Technology. We thank Aradhya Rajanala for encouraging the adoption of project-based learning in Classical Mechanics I in 2017. We thank C.A. Fair, C.K. Fair, J. Margolis, and C. Li for initial project work during the Classical Mechanics I course.

## Supplementary material

**Movie S1.** Evolution of experiment-simulation comparison.

The Supplementary Material is available at https://emergent-scientist.edp-open.org/10.1051/emsci/2024003/olm

## References

1. T. Dooling, J. Regester, M. Carnaghi, A. Titus, Am. J. Phys. **84**, 664–670 (2016)
2. M. Batista, Eur. J. Phys. **45**, 035001 (2024)
3. Z. Yan, H. Xia, Y. Lan, J. Xiao, Phys. Educ. **53**, 015011 (2018)
4. R. Cross, Phys. Teach. **61**, 568–571 (2023)
5. A. Agha, S. Gupta, T. Joseph, Am. J. Phys. **83**, 126–132 (2015)
6. S. Haddout, M. Rhazi, Eur. J. Comput. Mech. **24**, 302–318 (2015)
7. E. Etkina, A. Van Heuvelen, A. Karelina, R. Ruibal-Villasenor, D. Rosengrant, AIP Conf. Proc. **951**, 88–91 (2007)
8. R.J. Full, R. Dudley, M.A.R. Koehl, T. Libby, C. Schwab, Integr. Comp. Biol. **55**, 912–925 (2015)
9. B.R. Wilcox, H.J. Lewandowski, Phys. Rev. Phys. Educ. Res. **12**, 020132 (2016)
10. E.M. Smith, M.M. Stein, C. Walsh, N.G. Holmes, Phys. Rev. X **10**, 011029 (2020)
11. Z.Y. Kalender, E. Stump, K. Hubenig, N.G. Holmes, Phys. Rev. Phys. Educ. Res. **17**, 020128 (2021)
12. P.W. Irving, E.C. Sayre, Phys. Rev. ST Phys. Educ. Res. **11**, 020120 (2015)
13. D.R. Dounas-Frazer, J.T. Stanley, H.J. Lewandowski, Phys. Rev. Phys. Educ. Res. **13**, 020136 (2017)
14. V. Borish, J.R. Hoehn, H.J. Lewandowski, Phys. Rev. Phys. Educ. Res. **18**, 020135 (2022)
15. D. Kleppner, R. Kolenkow, An Introduction to Mechanics, 2nd edn. Cambridge University Press, Cambridge, UK, 2014
16. J. Levin, G. Perez-Giz, Phys. Rev. D **77**, 103005 (2008)
17. J. Healy, J. Levin, D. Shoemaker, Phys. Rev. Lett. **103**, 131101 (2009)
18. I. Gaponov, D. Popov, J.-H. Ryu, IEEE/ASME Trans. Mechatron. **19**, 1331–1342 (2014)
19. J.S. Brunner, J. Margolis, S. Tarr, D. Soto, D.I. Goldman, Bull. Am. Phys. Soc. **67**, (2022)
20. H. Ş. Kızılcık, M. Aygün, E. Şahin, N. Önder-Çelikkanlı, O. Türk, T. Taşkın, B. Güneş, Phys. Rev. Phys. Educ. Res. **17**, 023107 (2021)
21. A million to one, https://aeon.co/videos/ a-nobel-laureate-and-a-flea-circus-join-forces-for-an- unforgettable-demonstration-of-inertia
22. Frictional coefficient (reference) | Basic Bearing Knowledge, https://koyo.jtekt.co.jp/en/support/bearing-knowledge/8-4000.html
23. N.G. Holmes, H.J. Lewandowski, Phys. Rev. Phys. Educ. Res. **16**, 020162 (2020)
24. The Carnegie Classification of Institutions of Higher Education, Georgia Institute of Technology, https://carnegieclassifications.acenet.edu/index.php
25. Physics 4268/6268 Nonlinear Dynamics & Chaos, https://nldlab.gatech.edu/w/index.php?title=Main_Page
26. J. Aguilar, A. Lesov, K. Wiesenfeld, D.I. Goldman, Phys. Rev. Lett. **109**, 174301 (2012)

**Cite this article as:** Steven W. Tarr, Joseph S. Brunner, Emily Alicea-Muñoz, Daniel I. Goldman. The value of hands-on experiments in an upper-division classical mechanics course, Emergent Scientist **9**, 1 (2025), https://doi.org/10.1051/emsci/2024003

# Appendix A:

## A.1 Institutional Context

Our study began in author DIG's Spring 2021 offering of Classical Mechanics I, an upper-division course required for undergraduate physics majors at the R1 institution [24] Georgia Institute of Technology (GT). Roughly 35 second- and third-year students take the course every semester. The course is structured in a traditional lecture style with 2.5 contact hours per week plus optional office hours with the course instructor and a graduate teaching assistant (GTA). Assessments include weekly homework assignments (primarily from the textbook *An Introduction to Mechanics* by Kleppner and Kolenkow [15]), two take-home midterm exams, a semester-long group project, and a take-home final exam.

The course instructor added the group project in 2017 to encourage the development of hands-on experimental physics skills in upper-division students. By moving away from the "cookbook" approach to labs, the instructor could instead support students in designing, building, and conducting their own experiments and developing their own analysis methods [8]. The project structure was adapted from an analogous assignment used in the author's upper-division/graduate-level, lecture-style nonlinear dynamics course since 2010 [25]. The instructor introduces the group project around week 4 of the semester. Each group (3–5 students) must design and execute an experiment outside of class hours to analyze a principle of classical mechanics in their chosen system. The deliverables for the project are a 5-minute in-class proposal presentation, a 4-page proposal paper, a 15-minute in-class final presentation, and a 10-page final paper. Students are highly encouraged to consult with the instructor and GTA throughout the semester; groups also receive personal feedback at twice-monthly status reports during the lecture period. Across the four courses since 2017, 133 students created 38 unique project concepts (Fig. A.1). Example topics include physicalized textbook/exam problems, real-world systems (e.g., gymnastic techniques, bicycle stability, momentum conservation in hockey), and dynamically rich combinations of concepts (e.g. gyroscope on a pendulum, kinematics in viscous fluids).

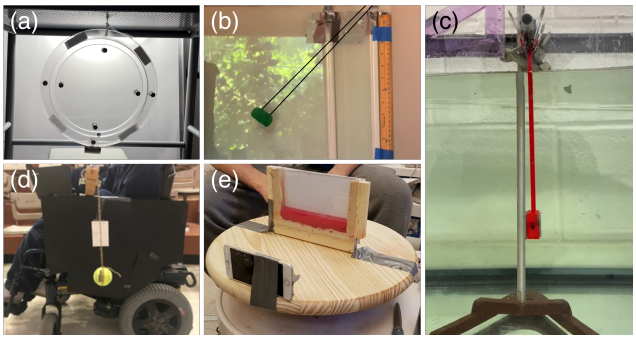


**Fig. A.1. Example student projects from Classical Mechanics I at GT**. (a) A bead travels along a confining circular track spun via a magnetic stirrer and settles at an equilibrium position dependent on angular velocity. (b) A student-fabricated ballistic pendulum (green modeling clay on strings) measures the muzzle velocity of a BB gun. (c) A pendulum suspended in liquid demonstrates damping dynamics dependent on fluid viscosity. (d) A pendulum mounted on a motorized wheelchair enables investigation of non-inertial reference frames. (e) A chamber of dyed water on a potter's wheel provides experimental confirmation of the predicted parabolic free-surface shape when spun.

Due to the COVID-19 pandemic, the Spring 2021 lectures occurred in a remote synchronous setting. The students who performed the project described in the main text elected to build a physical apparatus and meet in person for data collection. After finishing the course, students who demonstrated potential and drive for exceptional work were offered the opportunity to continue their study in the instructor's lab space. In rare cases, projects evolved into conference proceedings [19] and research publications [26].